Research Report

Realization of Fiber Lasing under Natural Sunlight Pumping

Shintaro Mizuno, Kazuo Hasegawa, Hiroshi Ito, Takenobu Suzuki and Yasutake Ohishi

Report received on Aug. 23, 2012

ABSTRACT We report a solar-pumped fiber laser (SPFL) using a double-clad Nd-doped fluoride fiber as the laser medium. The optical properties of Nd^{3+}-doped ZrF_4-BaF_2-LaF_3-AlF_3-NaF (ZBLAN) glass are evaluated. It has a high quantum efficiency, a large $\sigma_{se}\tau_r$ product, and a large integrated absorption strength. With an off-axis parabolic mirror that is 5 cm in aperture diameter, natural sunlight is concentrated by a factor of 10^4 and introduced into the ZBLAN fiber. A clear laser spectrum is obtained whose full-width-at-half-maximum is 0.013 nm at a peak wavelength of 1053.7 nm, with a low lasing threshold of 49.1 mW and a slope efficiency of 3.3%.

KEYWORDS Solar-pumped Laser, Fluoride Glass, ZBLAN, Quantum Efficiency, Double-clad Fiber

1. Introduction

A solar-pumped laser (SPL) converts incoherent sunlight with a wideband spectrum and low areal energy density into a monochromatic coherent optical beam. In recent years, SPLs have attracted attention for use in such technologies as satellite communications, space debris management, solar energy transmission from space to the earth, and energy cycling by conversion of sunlight into chemical energy.[1-3] The first solar-pumped laser oscillator was reported in 1963.[4] However, there remain many significant issues with such devices, including low laser efficiency, cooling, and poor beam quality.

Many of these issues can be dealt with by using fiber lasers made of glass materials. In this paper, we report fiber lasing using natural sunlight for the first time to the best of our knowledge. The geometry of the laser medium, the nature of the glass material, and the sunlight collecting optical system are investigated here for such a solar-pumped laser.

2. Components of a Solar-pumped Laser

2. 1 Geometry of the Laser Medium

Figure 1 shows the relationship between the normalized specific surface area, S/S_0, and the aspect ratio, $A = L/d$, of a cylindrical medium of length L and diameter d. Here S/S_0 is defined as the ratio of a surface area S of the laser material to the area S_0 when the aspect ratio is $A = 1$. An increase in the value of S/S_0 increases the cooling performance of the laser medium.

A rod laser medium has a value of A between 1 and 50 with $S/S_0 < 5$. On the other hand, when $S/S_0 > 10$, there are two geometries of interest: $A < 0.007$ corresponding to a disk laser medium, and $A > 4000$ corresponding to a fiber medium. These latter two geometries are best for solar-pumped lasers.

Consider the absorption of excitation light by the laser media. For a fiber geometry, owing to its long interaction length, it is possible to absorb almost all the light introduced into the fiber during its propagation in the longitudinal direction. On the other hand, for the thin disk geometry, it is difficult to absorb all the excitation light because of its short length. Consequently a fiber geometry is better suited for a solar-pumped laser.

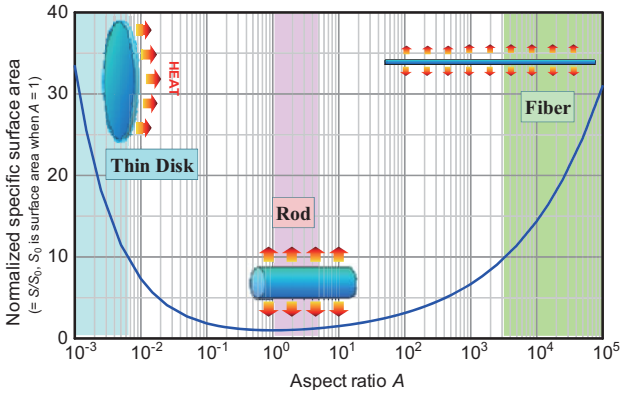

Fig. 1 Graph of S/S_0 as a function of the aspect ratio A.

2. 2 Oscillation Wavelength

Now consider the energy conversion efficiency from the input solar spectrum to the laser output. When an absorbed solar photon has energy larger than the energy of an emitted photon at the monochromatic lasing wavelength, the excess energy becomes converted to heat. On the other hand, a solar photon whose energy is smaller than that of the emitted laser photons is not absorbed and hence does not contribute to the lasing. The energy conversion efficiency η is given by

$$\eta = \frac{\int_{\lambda_S}^{\lambda_L} \frac{\lambda_i}{\lambda_L} I(\lambda_i)\, d\lambda_i}{\int_{\lambda_S}^{\lambda_e} I(\lambda_i)\, d\lambda_i}, \quad \cdots\cdots\cdots\cdots\cdots\cdots (1)$$

where λ_L is the lasing wavelength, λ_s and λ_e are the shortest and longest wavelengths of the solar spectrum, and $I(\lambda_i)$ is the spectral intensity of sunlight. Equation (1) measures the ratio of the absorbed energy at wavelengths below the lasing wavelength, accounting for the quantum defect due to the difference of wavelengths between the lasing and the excitation, to the incident energy of the solar spectrum at all wavelengths.

Figure 2 plots the energy conversion efficiency as a function of wavelength, calculated using Eq. (1) for air mass 1.5 (AM1.5) sunlight. The maximum conversion efficiency is about 49% at a wavelength near 1100 nm. An Neodymium-doped laser oscillates at around 1060 nm, near this maximum conversion efficiency. Lasing with an electronic transition $^4F_{3/2} \rightarrow {}^4I_{11/2}$ of Nd^{3+} ion proceeds according to a four-level scheme, leading to a low threshold. For that reason, Nd^{3+} is a promising active ion for solar-pumped lasers.

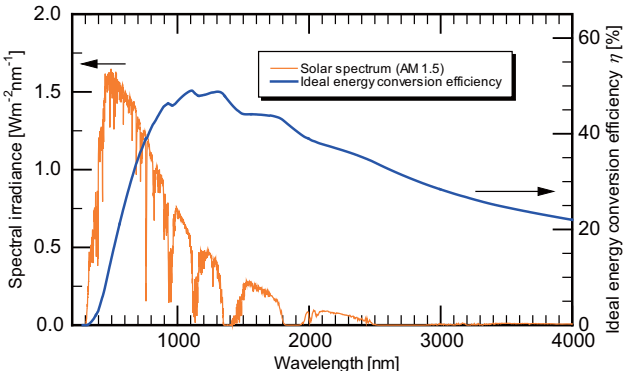

Fig. 2 Solar spectrum of AM1.5 and the resulting energy conversion efficiency.

2. 3 Laser Glass

Glass can be drawn into a fiber to serve as a laser medium. Nd-doped lasers have been used for nuclear fusion in fiber form. High-intensity lamps and laser diodes have been used as the excitation sources. However, the possibility of using a low-energy-pump source, such as sunlight, has not previously been considered. For this purpose, it is useful to clarify the optical properties of various Nd-doped glasses under solar irradiation. We investigated the optical properties of ZrF_4-BaF_2-LaF_3-AlF_3-NaF (ZBLAN) glass doped to varying extents with NdF_3.[5]

2. 3. 1 Absorption and Emission Cross Sections and Emission Lifetime of Nd:ZBLAN

ZBLAN glass, first created in 1975,[6] has a wide spectral window of transparency extending from about 0.22 to 8 μm.[7] Its loss is as low as 1 dB/km,[8] it has an effective phonon energy less than 600 cm^{-1},[9] and it tolerates doping levels of up to 10 mol.% of rare-earth ions.[7]

Figure 3 shows the absorption and emission cross sections of Nd-doped ZBLAN glass. The stimulated emission cross section was obtained from a Judd-Ofelt analysis,[10,11] which calculates the transition probabilities (or oscillator strengths) for the various transitions between the energy states of the rare-earth ions using a measured absorption spectrum. In turn, the absorption cross section can be calculated as

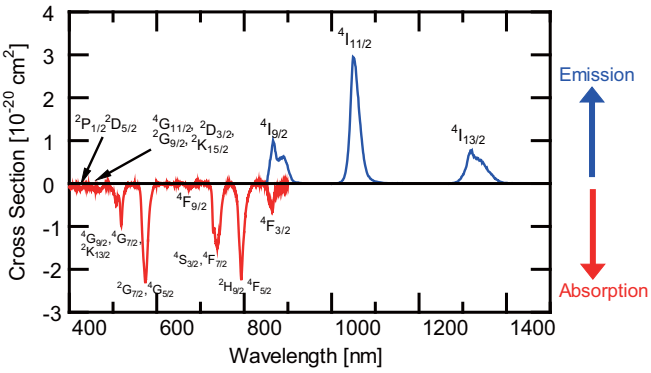

Fig. 3 Absorption and stimulated emission cross sections of Nd^{3+} doped in ZBLAN glass. The term symbols show the final state of the transitions. The initial states are $^4I_{9/2}$ for absorption and $^4F_{3/2}$ for emission.

$$\sigma_{abs}(\lambda) = \frac{\alpha_{Nd-doped}(\lambda) - \alpha_{undoped}(\lambda)}{n_{Nd}}, \quad \cdots\cdots (2)$$

where $\alpha_{Nd\text{-}doped}$ and $\alpha_{undoped}$ are the absorption coefficients for Nd-doped and undoped ZBLAN, respectively, and n_{Nd} is the concentration of Nd^{3+} ions in the doped sample. To evaluate the total absorption of sunlight by Nd-doped glasses, the cross section is then integrated across the 400–950 nm spectral region in which the glass is intended to be used, which is related to the absorption efficiency of broadband excitation sources.[12] The integrated absorption is listed in **Table 1**, relative to the value 1.583×10^{-18} cm^2·nm for ED-2 and LG670, a high-gain lithium calcium aluminosilicate glass.[12] The relative integrated absorption of Nd-doped ZBLAN is here found to be 0.91, which is only slightly lower than those of the silicate glass ED-2 and the phosphate glass LG750. Notably, it is larger than those of other fluoride glasses (ZBL, ZBN, and ZBLAN prepared by other researchers). This value suggests that our ZBLAN glass can absorb sunlight effectively. The stimulated emission cross section σ_{se} of the Nd^{3+} $^4F_{3/2} \rightarrow {}^4I_{11/2}$ transition at 1050 nm was $(2.95 \pm 0.18) \times 10^{-20}$ cm^2.

Figure 4 plots the measured radiative lifetime τ_r of the $^4F_{3/2}$ state of Nd^{3+} in ZBLAN as a function of the NdF_3 molar content x. Each lifetime was deduced from the e-folding time of an emission decay curve. The radiative lifetime is found to be 525 μs at low values of x, but it significantly decreases above 3 mol.% due to concentration quenching. The product of σ_{se} and τ_r is proportional to the slope efficiency and is inversely proportional to the threshold pump power of a laser. Therefore, it is a figure of merit for the laser transition. The product $\sigma_{se}\tau_r$ for the $^4F_{3/2} \rightarrow {}^4I_{11/2}$ transition of Nd^{3+} for several glasses is listed in Table 1. The value of $\sigma_{se}\tau_r$ for ZBLAN is here found to be $(1.45 \pm 0.19) \times 10^{-23}$ cm^2·s. This value is twice as large as that of Al-doped silica glass and is comparable to that of LG750.

Table 1 Stimulated emission cross section σ_{se}, radiative lifetime τ_r, and product $\sigma_{se}\tau_r$ for Nd^{3+} at the $^4F_{3/2} \rightarrow {}^4I_{11/2}$ transition, together with the relative integrated absorption of Nd^{3+} in the 400–950 nm wavelength range.

Glass	σ_{se} [10^{-20} cm^2]	τ_r [μs]	$\sigma_{se}\tau_r$ [10^{-23} cm^2·s]	Relative Absorption
Al-doped silica [a]	1.5	500	0.75	–
ED-2 (LG-670) [b]	2.7	359	0.97	1
LG750 [b]	4.0	352	1.41	1.11
ZBL [b]	3.0	446	1.34	0.78
ZBN [b]	2.9	434	1.26	0.79
ZBLAN [c]	3.17	444	1.41	–
ZBLAN [d]	3.06±0.17	460	1.41	0.79
ZBLAN [e]	3.4	394	1.36	–
ZBLAN [f]	2.95±0.18	496±38	1.45±0.19	0.91

a: Ref. (6), *b*: Ref. (7), *c*: Ref. (8), *d*: Ref. (9), *e*: Ref. (10), *f*: This work

2. 3. 2 Optical Quantum Efficiency

To quantify the optical properties of glass under solar illumination, a measurement system was constructed to determine the quantum efficiency (QE) using an integrating sphere and different excitation sources, as illustrated in **Fig. 5**. An altazimuth mount on a tripod was used to track the sun automatically. The sunlight was focused onto the tip of an optical fiber bundle by a lens with a focal length of 100 mm and a diameter of 50 mm. Alternatively, laser light could be coupled through another fiber into the integrating sphere for comparison with the solar spectrum. Two different photonic multichannel analyzers (PMAs) were used sequentially as spectrometers and detectors for the measurements. One is a visible PMA (Hamamatsu C9220-02) covering the wavelength range of 200–950 nm with a resolution of 2 nm, and the other is a near-infrared PMA (Ohtsuka Denshi Photal MCPD-5000) covering the wavelength range of 900–1600 nm with a resolution of 3.4 nm. The spectral sensitivities of these PMAs were calibrated with standard light sources by the manufacturers. The QE measurement for each sample was completed within 2 minutes. The step-by-

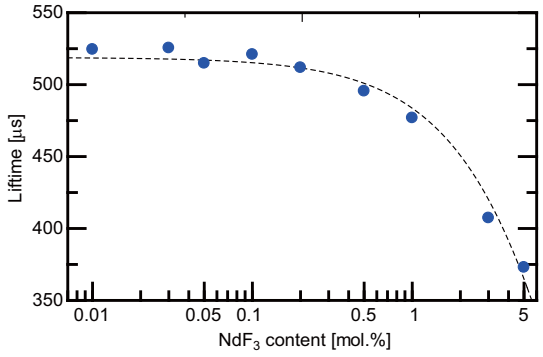

Fig. 4 Measured radiative lifetime of the $^4F_{3/2}$ state of Nd^{3+} in ZBLAN glass as a function of the NdF_3 molar content x. The dashed curve is a guide to the eye.

step procedure for the measurement is described elsewhere.[17]

Panel (a) of **Fig. 6** shows the spectral intensities measured using the integrating sphere with and without a ZBLAN glass sample of $x = 0.5$ mol.% under sunlight irradiation, and panel (b) shows the difference spectrum. Sharp absorption and emission lines due to Nd^{3+} can be seen. Although broad host absorption bands (including defects and impurities) occur for Nd-doped borosilicate glass,[17] they appear to be negligibly small for ZBLAN glass.

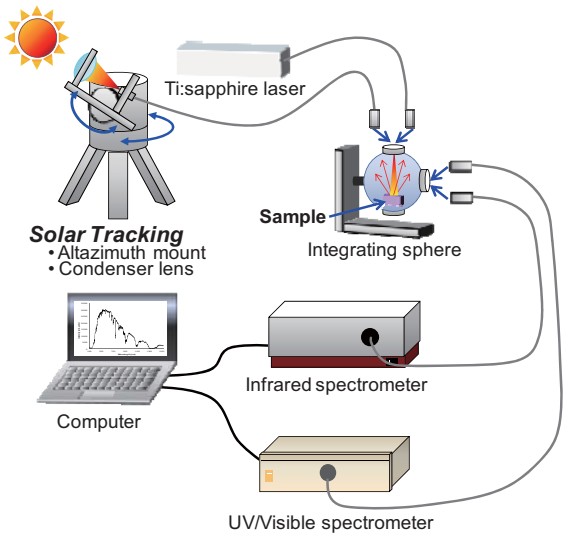

Fig. 5 System for measuring optical quantum efficiency using an integrating sphere.

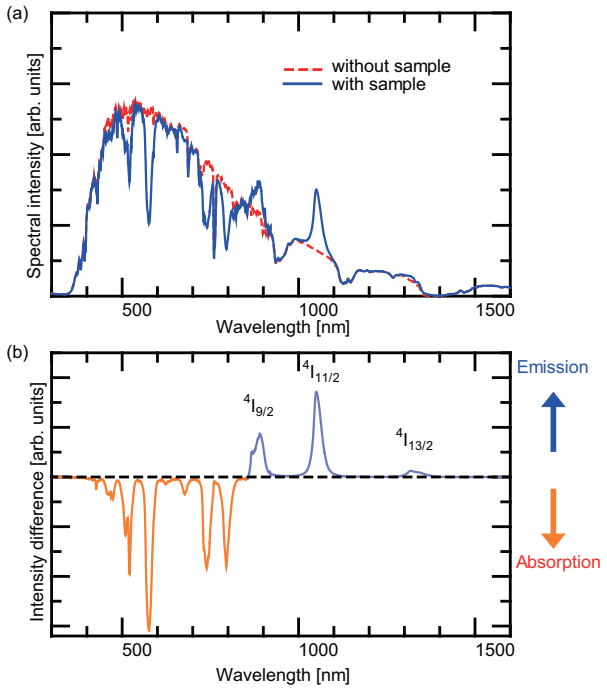

Fig. 6 (a) Spectral intensity of a 0.5 mol.% Nd-doped ZBLAN glass sample (solid curve) and background intensity without the sample (dotted curve) under sunlight irradiation. (b) Difference spectrum with and without the sample.

Figure 7 plots the radiative QE (η_r) of the $^4F_{3/2}$ state of Nd^{3+} and the internal quantum efficiency under 793-nm excitation from a Ti:sapphire laser (η_{793}) and under sunlight illumination (η_{ns}) as a function of the molar content x of NdF_3. The radiative QE is calculated from the measured radiative lifetime and the result of Judd-Ofelt analysis. Its value is found to be 100% (within error bars) below $x = 0.5$ mol.%, implying that nonradiative decay is negligible. However, η_r decreases with increasing x above 3%, due to concentration quenching. For 793-nm excitation, the QE is as high as 88% in the low x region, comparable to the value of 90% measured for a Czochralski-grown Nd^{3+}:YAG crystal with 514.5-nm excitation.[18] Again, η_{793} decreases with increasing x, becoming 25% at $x = 5\%$ due to concentration quenching. Finally, η_{ns} has a maximum value of 70% at $x = 0.5$ mol.% and it decreases with increasing x. However, η_{ns} also decreases with decreasing x at low values of x, in striking contrast to η_r and η_{793}. The probable explanation is as follows. When x decreases, the Nd absorption decreases, while the host glass absorption remains constant. Although the absorption coefficient of the ZBLAN glass is small, it is not zero, and therefore at low concentrations, the ratio of the absorption by the active ions and by the host (which does not contribute to the emission) decreases, resulting

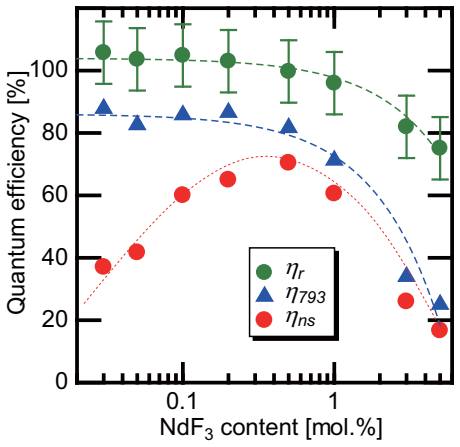

Fig. 7 Optical quantum efficiencies of Nd-doped ZBLAN glass as a function of the NdF_3 molar content x.

in a decrease in quantum efficiency.

Nonradiative relaxation of excited rare-earth ions is usually attributed to multiphonon emission and to concentration quenching by energy migration between rare-earth ions or by energy transfer to hydroxyl (-OH) groups. The nonradiative relaxation rate via multiphonon emission is given by[19]

$$W_{mp} = C\left\{\left[\exp\left(\frac{\hbar\omega}{kT}\right)-1\right]^{-1}+1\right\}^{p}\exp\left(-\alpha\Delta E\right), \quad \cdots\cdots\cdots\cdots\cdots (3)$$

where C is a constant characteristic of the host material, $\hbar\omega$ is the energy of the phonon, ΔE is the energy gap between the states, $p = \Delta E/\hbar\omega$ is the number of phonons emitted in the process, k is Boltzmann's constant, T is temperature, and α is a host-dependent parameter related to the electron-phonon coupling strength. Equation (3) implies $W_{mp} \approx 0.6\ s^{-1}$ for Nd^{3+}: ZBLAN starting from state $^4F_{3/2}$, using the parameters $C = 1.6 \times 10^{10}\ s^{-1}$, $\alpha = 5.2 \times 10^{-3}\ cm^{-1}$,[20] and $\hbar\omega = 600\ cm^{-1}$. The radiative and nonradiative decay rates of several Nd-doped glasses are summarized in **Table 2**. The emission lifetime of the $^4F_{3/2}$ state of Nd^{3+} in ZBLAN glass is 496 μs, so that the spontaneous emission rate $A_r \equiv 1/\tau_r$ is 2016 s^{-1}. In comparison to this value, the nonradiative relaxation rate by multiphonon emission is small. The glasses were prepared in a dry atmosphere, and absorption bands due to hydroxyl (-OH) were not observed in our samples in the near-infrared region. For this reason, nonradiative relaxation by energy transfer to hydroxyl is negligible. The nonradiative relaxation in the limit of zero concentration by multiphonon emission, W_0, is also negligible for Nd-doped ZBLAN.[21] Therefore the quantum efficiency $A_r/(A_r + W_0 + W_{OH})$ should be nearly 100% for low x values, in good agreement with the results for η_r in Fig. 7.

Table 2 Relaxation parameters for several Nd-doped glasses.

Glass	A_r [s^{-1}]	W_0[s^{-1}]
Borosilicate [a]	2850	2095
LG750 [b]	2425	216±150
ZBLAN [c]	1922	0
ZBLAN [d]	2016±145	0

a: Ref. (17), *b*: Ref. (22), *c*: Ref. (21), *d*: This work

The results of the above study indicate that ZBLAN glass is a promising solar-pumped fiber laser medium. A prototype Nd-doped ZBLAN glass fiber was consequently fabricated, and it demonstrated natural-sunlight-pumped laser oscillation, as described next.

3. Laser Properties of a Solar-pumped Fiber Laser

Figure 8 shows a diagram of the solar-pumped fiber laser (SPFL) experiment. An off-axis parabolic mirror is used to concentrate the light because it is free from chromatic aberration and provides a relatively high concentration. The concentration ratio is estimated to be 10626. Sunlight was focused onto the tip of a double-clad fiber of Nd-doped ZBLAN having a mode field diameter of 5 μm, an inner cladding diameter of 123 μm, a cladding numerical aperture (NA) of 0.5, reflecting mirrors of 98.0% at 1050 nm, and a length of 7.5 m. Whereas other solar-pumped lasers require forced cooling of the medium, an SPFL can operate without one. The optical system is mounted on an altazimuth mount.

Lasing pumped by natural sunlight was operated under clear skies with occasional cumuli clouds. **Figure 9** plots the spectra of the sunlight before and after passing through the Nd-doped ZBLAN fiber. The direct solar spectrum is calculated by Bird's model.[23] Standard conditions defined in ISO and JIS are used, except for the local value of TOYOTA Central R&D Laboratories of 35 degrees 10 minutes north latitude and 137 degrees 3 minutes east longitude. The spectral intensity in Bird's model is corrected based on the measured spectral intensity after transmission through the fiber and a resonator mirror, and losses of the ZBLAN fiber measured by cutback technique.

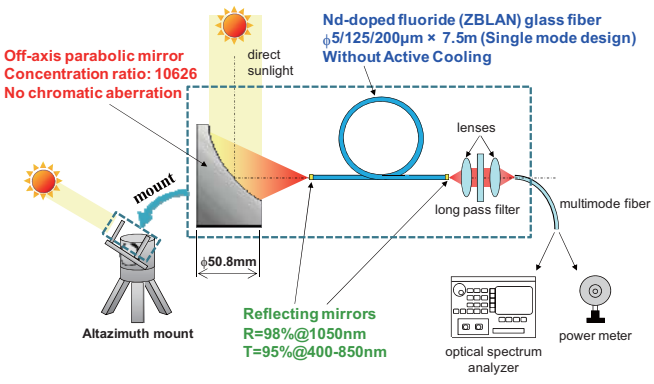

Fig. 8 Schematic of the solar-pumped fiber laser experiment.

The laser line is evident as the sharp spike near 1050 nm in Fig. 9. Broader absorption bands at peak wavelengths of about 420, 458, 521, 575, 650, 688, 740, 795 and 867 nm are attributed to the electronic transitions of $^4I_{9/2} \rightarrow (^2P_{1/2}, {}^2P_{5/2})$, $^4I_{9/2} \rightarrow (^4G_{11/2}, {}^2D_{3/2}, {}^2G_{9/2}, {}^2K_{15/2})$, $^4I_{9/2} \rightarrow (^4G_{9/2}, {}^4G_{7/2}, {}^2K_{13/2})$, $^4I_{9/2} \rightarrow (^4G_{7/2}, {}^4G_{5/2})$, $^4I_{9/2} \rightarrow {}^2H_{11/2}$, $^4I_{9/2} \rightarrow {}^4F_{9/2}$, $^4I_{9/2} \rightarrow (^4S_{3/2}, {}^4F_{7/2})$, $^4I_{9/2} \rightarrow (^2H_{9/2}, {}^4F_{5/2})$, and $^4I_{9/2} \rightarrow {}^4F_{3/2}$ of Nd^{3+}. Almost all of the sunlight is absorbed near 521, 575, 740, 795, and 867 nm. In contrast, strong transmission is observed for blue light at 410–510 nm, red light at 590–725 nm, and near-infrared light from 890 nm up to the lasing wavelength. Improved efficiency for solar energy conversion would result if a sensitizer were used that absorbs sunlight in these spectral regions.

Figure 10 expands the lasing spectra at different times, revealing a dense set of peaks that vary considerably in amplitude, partly because of inhomogeneous broadening of the Nd^{3+} ions in the glass and because of longitudinal-mode hopping. All of the spectra have a peak around 1053 nm, but many other lines between 1052 and 1054 nm are also observed. In at least one instance, the full-width-at-half-maximum of the laser line peaking at 1053.7 nm is 0.013 nm.

Figure 11 plots the output power P_{out} of the SPFL versus the input solar power P_{in} captured into the inner cladding of the fiber. The input power to the parabolic mirror was calculated by multiplying the 0.737 which is ratio of the direct solar radiation I_{DIR} to global solar radiation I_G. The value of I_G was measured using an illuminance meter. In turn, the ratio of I_{DIR} to I_G was calculated from the relation $I_{DIR} = I_G - I_{DIF}$ where I_{DIF} is the diffuse solar radiation calculated from the measured value of the ratio of I_{DIF} to I_G.

The diameter d_{sun} of the image of the sun formed by the parabolic mirror was about 500 µm, obtained as the distance between the two points where the measured power falls to $1/e^2$ by the knife-edge method. Then P_{in} was calculated as I_{DIR} ($d_{inn}{}^2$ / $d_{sun}{}^2$) where d_{inn} is the diameter of the inner cladding of the fiber. The maximum output power was measured to be 0.57 mW at 65.0 mW pumping. The lasing threshold occurred at 49.1 mW input solar power. The slope efficiency for a single-sided fiber output above threshold was 3.3%, whereas the overall efficiency was 0.88%. Because the reflectivity at both ends of the fiber is identical, the output power from the other side should be the same,

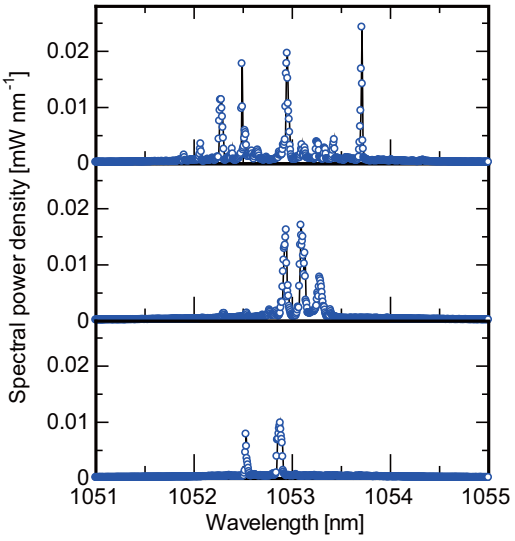

Fig. 10 Lasing spectra measured a few minutes apart.

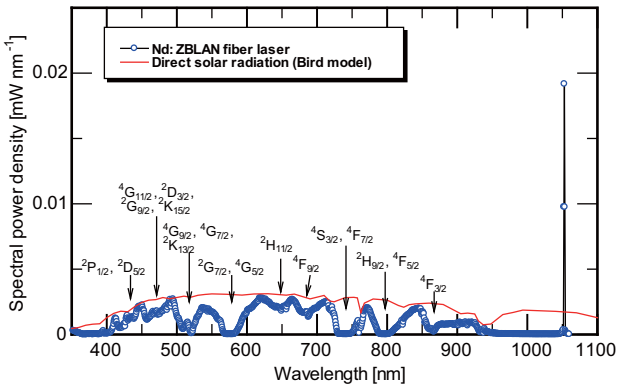

Fig. 9 Spectra of sunlight before and after passage through the Nd-doped ZBLAN fiber.

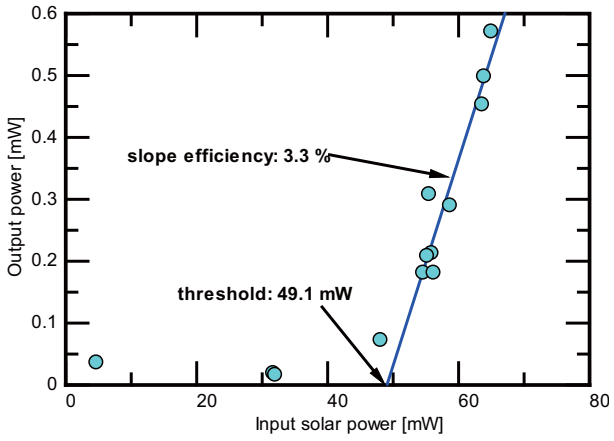

Fig. 11 Output power of the solar-pumped fiber laser as a function of the input power.

thereby doubling the slope efficiency and total efficiency to 6.6% and 1.76%, respectively.

Further improvements in the efficiency of SPFL can be obtained from: (1) optimization of the reflecting mirrors, (2) improvement of the absorption of the sunlight, and (3) reduction of losses in the laser cavity from the fiber and mirrors. Regarding the output power of the SPFL, which was only 0.57 mW in the present work, it could be improved by using a fiber bundle.

4. Conclusion

The operation of a solar-pumped fiber laser (SPFL) has been demonstrated for the first time using concentrated natural sunlight and a Nd-doped ZBLAN (fluoride glass) fiber. Optical parameters relevant to the design of the laser were evaluated for Nd:ZBLAN. The stimulated emission cross section of the ${}^4F_{3/2} \rightarrow {}^4I_{11/2}$ transition is $\sigma_{se} = 2.96 \times 10^{-20}$ cm^2, and the radiative lifetime obtained from a Judd-Ofelt analysis is $\tau_r = 496$ μs. Their product is $\sigma_{se}\tau_r = 1.45 \times 10^{-23}$ cm^2·s, which is the largest found for Nd^{3+} doped in glasses. The integrated absorption strength in the 450–900 nm region of Nd-doped ZBLAN glass was also the largest among Nd^{3+} doped fluoride glasses. These results show that Nd-doped ZBLAN glass is one of the most promising gain media for solar-pumped lasers. A prototype Nd:ZBLAN fiber was consequently fabricated and used in a demonstration of natural-sunlight-pumped laser oscillation. An off-axis parabolic mirror was used as a concentrator. With a measured threshold of 49.1 mW, the slope efficiency was estimated to be 6.6% and the overall efficiency to be 1.76%. The realization of an SPFL using a double-clad single-mode fiber overcomes issues of beam quality, cooling, and energy conversion efficiency. It opens the way for compact solar-pumped lasers, in contrast to previous large high-power systems.

References

(1) Young, C. G., "A Sun-pumped cw One-watt Laser", *Appl. Opt.*, Vol.5, No.6 (1966), pp.993-997.

(2) De Young, R. J., "Beam Profile Measurement of a Solar-pumped Iodine Laser", *Appl. Opt.*, Vol.25, No.21 (1986), pp.3850-3854.

(3) Yabe, T., et al., "100 W-class Solar Pumped Laser for Sustainable Magnesium-hydrogen Energy Cycle", *J. Appl. Phys.*, Vol.104, No.8 (2008), 083104.

(4) Kiss, Z. J., et al., "Sun Pumped Continuous Optical Maser", *Appl. Phys. Lett.*, Vol.2, No.5 (1963), pp.93-94.

(5) Suzuki, T., et al., "Spectroscopic Investigation of Nd^{3+}-doped ZBLAN Glass for Solar-pumped Lasers", *J. Opt. Soc. Am. B*, Vol.28, No.8 (2011), pp. 2001-2006.

(6) Poulain, M., et al., "Verres Fluores au Tetrafluorure de Zirconium Proprieties Optiques d'un verre Dope au Nd^{3+}", *Mat. Res. Bull.*, Vol.10, No.4 (1975), pp.243-246.

(7) Zhu, X. and Peyghambarian, N., " High-power ZBLAN Glass Fiber Lasers: Review and Prospect", *Adv. Opt. Electron.*, Vol.2010 (2010), 501956.

(8) Kanamori, T. and Sakaguchi, S., "Preparation of Elevated NA Fluoride Optical Fibers", *Jpn. J. Appl. Phys.*, Vol.25 (1986), pp.L468-L470.

(9) Gan, F., "Optical Properties of Fluoride Glasses: A Review", *J. Non-Cryst. Solids*, Vol.184, No.1 (1995), pp.9-20.

(10) Judd, B. R., "Optical Absorption Intensities of Rare-earth Ions", *Phys. Rev.*, Vol.127, No.3 (1962), pp.750-761.

(11) Ofelt, G. S., " Intensities of Crystal Spectra of Rare-earth Ions", *J. Chem. Phys.*, Vol.37, No.3 (1962), pp.511-520.

(12) Stokowski, S. E., et al., *Nd-doped Laser Glass Spectroscopic and Physical Properties*, *Technical Report M-095* (1981), Lawrence Livermore National Laboratory.

(13) Arai, K., et al., "Aluminum or Phosphorus Co-doping Effects on the Fluorescence and Structural Properties of Neodymium-doped Silica Glass", *J. Appl. Phys.*, Vol.59, No.10 (1986), pp.3430-3436.

(14) Takebe, H., et al., "Spectroscopic Properties of Nd^{3+} and Pr^{3+} in Gallate Glasses with Low Phonon Energies", *Appl. Opt.*, Vol.36, No.24 (1997), pp.5839-5843.

(15) Tesar, A., et al., "Optical Properties and Laser Parameters of Nd^{3+}-doped Fluoride Glasses", *Opt. Mater.*, Vol.1, No.3 (1992), pp.217-234.

(16) Miniscalco, W. J., "Optical and Electronic Properties of Rare Earth Ions in Glasses", *Rare Earth Doped Fiber Lasers and Amplifiers, ed., Digonnet, M. J. F.* (2001), pp.17-112, Taylor & Francis.

(17) Suzuki, T., et al., "Quantum Efficiency Measurements on Nd-doped Glasses for Solar Pumped Lasers", *J. Non-Cryst. Solids*, Vol.356, No.44-49 (2010), pp.2344-2349.

(18) Devor, D. P., et al., "Nd:YAG Quantum Efficiency and Related Radiative Properties", *IEEE J. Quantum Electron.* Vol.25 (1989), pp.1863-1873.

(19) Layne, C. B., et al., "Multiphonon Relaxation of Rare-earth Ions in Oxide Glasses", *Phys. Rev. B*, Vol.16, No.1 (1977), pp.10-20.

(20) Reisfeld, R. and Jørgensen, C. K., "Excited State Phenomena in Vitreous Materials", *Handbook on the Physics and Chemistry of Rare Earths*, Vol.9 (1987), pp.1-90, Elsevier.

(21) Jacinto, C., et al., "Normalized-lifetime Thermal-lens Method for the Determination of Luminescence Quantum Efficiency and Thermo-optical Coefficients: Application to Nd^{3+}-doped Glasses", *Phys. Rev. B*,

Vol.73, No.12 (2006), 125107.
(22) Caird, J. A., et al., "Quantum Efficiency and Excited-state Relaxation Dynamics in Neodymium-doped Phosphate Laser Glasses", *J. Opt. Soc. Am. B*, Vol.8, No.7 (1991), pp.1391-1403.
(23) Bird, R. E. and Riordan, C., "Simple Solar Spectral Model for Direct and Diffuse Irradiance on Horizontal and Tilted Planes at the Earth's Surface for Cloudless Atmospheres", *J. Climate Appl. Meteor.*, Vol.25, No.1 (1986), pp.87-97.

Shintaro Mizuno
Research Fields:
- Solar Energy Conversion
- Solar-pumped Fiber Laser
- Inorganic Materials/Physical Properties

Academic Degree: Dr.Eng.
Academic Societies:
- The Japan Society of Applied Physics
- The Ceramic Society of Japan

Kazuo Hasegawa
Research Fields:
- Solar Energy Conversion
- Laser Engineering
- Electromagnetic Wave Theory

Academic Degree: Dr.Eng.
Academic Societies:
- IEEE Photonics Society
- The Japan Society of Applied Physics
- Optical Society of Japan

Hiroshi Ito
Research Fields:
- Solar-pumped Laser
- Solar Energy Conversion
- Optical Measurement System

Academic Society:
-The Japan Society of Applied Physics

Takenobu Suzuki*
Research Field:
- Optoelectronic Materials Science and Engineering

Academic Degree: Dr.Eng.
Academic Societies:
- The Japan Society of Applied Physics
- The Ceramic Society of Japan
- The Laser Society of Japan
- The American Ceramic Society
- Materials Research Society
- The Optical Society of America
- SPIE

Yasutake Ohishi*
Research Field:
- Photonics

Academic Degree: Ph.D.
Academic Societies:
- The Optical Society of America
- IEEE Photonics Society
- Institute of Electronics, Information and Communication Engineers (IEICE)
- The Japan Society of Applied Physics
- The Ceramics Society of Japan

Awards:
- Best Paper Award of IEICE, 1994
- Best Paper Award of 2nd Optoelectronics & Communications Conference (OECC), 1997
- Sakurai Award of Optoelectronic Industry and Technology Development Association (OITDA), 1997
- Electronics Society Award of IEICE, 1998
- Achievement Award of IEICE, 2001
- Academic Award of the Ceramic Society of Japan, 2007

*Toyota Technological Institute